Vacancies and Electron Deficient Surface Anions on the Surface of MgO Nanoparticles

M. Sterrer, O. Diwald, and E. Knözinger*

Institut für Physikalische und Theoretische Chemie, Technische Universität Wien, Veterinärplatz 1, Trakt GA, A-1210, Wien, Austria

Received: November 5, 1999; In Final Form: January 20, 2000

In the course of surface defect characterization on MgO nanoparticles three different types of O^- species were observed by electron paramagnetic resonance (EPR) spectroscopy. They are a result of UV excitation under high-vacuum conditions/in O_2 atmosphere or of surface color center bleaching by N_2O, respectively. On the other hand, the O^- species induce homolytic H_2 splitting which was evidenced for the first time by infrared (IR) spectroscopy. The resulting products are a so far unknown IR active OH group and an uncharged surface mobile H atom. The latter one acts as a reducing agent for either one of two types of anion vacancies which are transformed into EPR active surface color centers F_S^+. They are fundamentally different from the classical F_S^+(H) center obtained in predominant abundance by UV irradiation of MgO in H_2 atmosphere. One of the above-mentioned O^- species is created by bleaching of F_S^+(H) by N_2O. The respective EPR signal is exactly the same as that obtained by thermal decomposition of a surface ozonide species which was produced by UV induced O_2 chemisorption at a single cation vacancy. Thus, one may conclude that the classical F_S^+(H) center has to be related to a cation−anion divacancy.

Introduction

Defective surface sites on MgO particles have been the subject of considerable experimental[1,2] and theoretical[3−6] interest over more than 3 decades. This is due to the important role of earth alkaline oxides—in pure form or in oxide mixtures—in heterogeneous catalysis, i.e., more specifically in oxidative coupling of methane (OCM). It has been suggested that both low-coordinated (LC) anion and cation sites,[7,8] anion vacancies (F_S^{2+}),[9,10] and electron deficient oxide ions (O^-)[11] are somehow involved in this complicated and not yet definitely elucidated system of reaction steps.

Paramagnetic O_S^- (the subscript "S" indicates a location in the surface) are capable of radical cleavage processes, such as the hydrogen abstraction from methane molecules interacting with the oxide surface.[12] They are also responsible for significant UV induced homolytic hydrogen splitting. This was studied extensively by means of electron paramagnetic resonance (EPR) and temperature programmed desorption (TPD) techniques.[13] The $(O_S)^-$ species were obtained in different ways, e.g., by excitation of low-coordinated surface anions by UV light[7,14−17] or by "filling" of anion vacancies with paramagnetic O^- species.[18,19] In both types of experiments high surface area MgO samples obtained by controlled thermal decomposition of the corresponding hydroxide were used.[12−19]

UV excitation changes exclusively the electronic structure, whereas the geometric arrangement of the ions remains untouched.[20] UV/vis diffuse reflectance data of chemical vapor deposition (CVD) MgO[21] reveal two absorption bands at 230 and 270 nm. According to the model of Garrone et al.[7] the corresponding energies of 5.75 eV (230 nm) and 4.62 eV (270 nm) are assigned to charge-transfer transitions in surface ion pairs with four- and three-coordinated anions, respectively:

$$(O_{LC}^{2-})_S + h\nu_{UV} \rightarrow (O_{LC}^{-})_S + e^- \quad (1)$$

where "LC" denotes the low-coordinated surface anions. It should be emphasized here that the electron appearing in eq 1 is always—at least partially—attached to an electron acceptor. Under vaccum conditions a short-lived charge-transfer complex $O^- Mg^+$ is formed in the excitation step.[7] If O_2 gas is present during the irradiation, the transferred electron can be captured:[14−16]

$$e^- + O_2 \rightarrow O_2^- \quad (2)$$

The resulting superoxide anion (O_2^-) is then complexed by a surface cation. Another effect of the presence of O_2 is the UV induced formation of ozonide:[17]

$$O_S^{2-} + O_2 + h\nu_{UV} \rightarrow O_3^- + e^- \quad (3)$$

The ozonide anions O_3^- are also paramagnetic surface species and, therefore, EPR active.

The "filling" of anion vacancies with O^- comprises two steps, namely, formation of surface color centers and subsequently the process of bleaching them by N_2O.[18,19]

$$F_S^{2+} + h\nu \xrightarrow{H_2} F_S^+(H) \quad (4)$$

$$F_S^+(H) + N_2O \rightarrow O_S^- + N_2\uparrow \quad (5)$$

Only recently a hypothesis regarding the location of the anion vacancies which are involved in the process described by eqs 4 and 5 was brought forward.[22] The oxygen vacancies which survive the thermal treatment at temperatures above 1120 K are likely to be positioned in corners and edges.[22,23] This is confirmed by quantum chemical calculations which reveal a general trend in the stability of the different types of vacancies. Low-coordinated ones are more stable than their analogues with

* To whom correspondence should be addressed. E-mail: knoezing@fbch.tuwien.ac.at.

10.1021/jp993924l CCC: $19.00
Published on Web 03/24/2000

higher coordination.[5] O_S^- species resulting from the "filling" procedure should, therefore, preferentially be three- or four-coordinated.

The EPR spectrum of the O^- ion mainly consists of two resonance components $g_\perp$ and $g_\parallel$ related to a uniaxial symmetry of the respective ion on the surface. In a first-order approximation,[24,25] these values are given by

$$g_\parallel \approx g_e$$
$$g_\perp = g_e + (2\lambda/\Delta E) \quad (6)$$

where g_e is the free spin value, λ is the spin−orbit coupling constant of oxygen, and ΔE is the energy difference between the p_z level containing the electron hole and the two degenerate p_x and p_y levels. ΔE reflects the local crystal field at the surface site.

The present paper aims at the discrimination of different types of electron deficient anions $(O^-)_S$ on the surface of nanometer-sized MgO, which was obtained by chemical vapor deposition (CVD).[26] As shown by previous experiments this material exhibits a comparatively high concentration of both low-coordinated surface ions and surface vacancies. It is, therefore, particularly well-suited for the identification and characterization of O_S^- species by EPR and FTIR spectroscopy. The two different procedures of O_S^- production (see above) will, of course, play a prominent role in the present study and should contribute to a better understanding of the reactive interplay between anion vacancies and low-coordinated surface sites.

Experimental Section

All experiments were carried out with the same type of MgO obtained by chemical vapor deposition in a flow system.[27] As starting material high-purity Mg pieces supplied by Johnson Matthey GmbH were used. The specific surface area of the resulting MgO material determined by BET measurements is around 400 m^2/g. To get a totally de-hydroxylated surface, the sample was gradually annealed at 1173 K under dynamic vacuum ($<10^{-5}$ mbar) before each experiment. This leads to a reduction of the specific surface area to 320 m^2/g. The rate of temperature increase for the annealing steps was 10 K/min. All samples were treated at 870 K with oxygen in order to burn organic contaminants originating from the oil of the vacuum pumps used in the flow system. The gases H_2 (99.999%) and $^{16}O_2$ (99.998%) for adsorption studies were provided by Messer Griesheim. A 300 W Xe lamp (Oriel) was applied for UV irradiation. The light beam passes through a water filter in order to avoid sample heating by IR irradiation. All UV excitation experiments on MgO were carried out at room temperature. The exposure time amounted to 10 min in oxygen atmosphere and to 30 min in vacuo or in hydrogen (100 mbar, color center formation).

The IR and EPR sample cells are connected to an appropriate high-vacuum pumping rack. It allows thermal activation of the sample at less than 10^{-5} mbar and adsorption/desorption experiments with diverse gases. For the IR experiments small quantities of MgO powder (20−30 mg) were pressed into pellets of around 50 mg/cm^2. The pressure applied was less than 10 bar and did not initiate any change of the specific surface area. For the EPR experiments similar amounts of the MgO sample batch also used for IR spectroscopy was filled in EPR tubes.

The IR spectra were recorded using a Fourier transform IR spectrometer model IFS 113v (Bruker Optik GmbH). The resolution was 3 cm^{-1}. A set of 300 interferogram scans was averaged in order to guarantee a reasonable signal-to-noise ratio. The reference for the absorbance spectra is a MgO sample previously subjected to thermal activation and then cooled to room temperature. The EPR spectra were recorded using a Bruker EMX 10/12 spectrometer system in the X band. The color center signals were obtained at room temperature in one scan, whereas the spectra presenting paramagnetic oxygen species required a reduction of the temperature to 77 K in order to improve resolution. In this case 10 co-added spectra sufficed to obtain a satisfactory signal-to-noise ratio. The DPPH signal as well as the lines originating from traces of Mn^{2+} in the sample were applied for the g value calibration.

Results

(1) Homolytic H_2 Splitting. Previous IR studies in our own laboratory provided unambiguous evidence for two different heterolytic H_2 splitting mechanisms on the surface of thermally activated (1170 K) CVD MgO.[27] They give rise to two pairs of OH and MgH stretching bands.[29,30] If the H_2 chemisorption occurs under UV irradiation, additional OH stretching bands appear. Three of them were assigned to surface OH groups which interact via H bonds with surface color centers as proton acceptors[31] originating from a UV induced electron transfer from hydride groups to surface anion vacancies. Furthermore the UV irradiation creates an additional OH stretching band at 3698 cm^{-1}, which is essentially absent in the dark reaction (Figure 1a). Both position and width of the band at 3698 cm^{-1} point at an essentially free and isolated OH group. An intensity correlated counterpart in the MgH stretching region—as an evidence of a heterolytic H_2 splitting—has not been observed. At room temperature the band is formed irreversibly. Different from OH bands which are related to an interaction with surface color centers in the immediate environment, the 3698 cm^{-1} band is not sensitive to the presence of O_2.

On the other hand, the band also appears—even though weaker than during the H_2 chemisorption under UV irradiation (Figure 1c)—if the MgO sample first exposed to UV light in the presence of O_2 is then subjected to vacuum and finally to H_2 gas in the dark (Figure 1b). Obviously the O_2 molecules stabilize the short-lived, low-coordinated (O_S^-) species, which—as radical anions—are able to initiate the homolytic H_2 splitting. The interference of spurious amounts of H_2O in the IR cell may definitely be excluded. All traces presented in Figure 1 are difference spectra resulting from ratioing the spectral data obtained after chemisorption against those before. None of the background spectra provided any clues to the presence of H_2O or its chemisorption products on the surface.

To get further insight into the chemical and physical properties of the surface species provoking the formation of the OH groups related to the OH bands at 3698 cm^{-1}, complementary EPR studies were performed.

(2) Transformation of Surface Anions into Paramagnetic Centers. The EPR spectrum of paramagnetic species obtained after 1 h of UV irradiation ($\lambda > 200$ nm, no UV light during the EPR measurement) at room temperature and dynamic vacuum is presented in Figure 2. According to the axial symmetry of the crystal field of the corresponding spin center, two components with $g_\perp = 2.036$ and $g_\parallel = 2.002$ were observed. In agreement with literature data they are related to an electron deficient surface oxygen anion O_S^- which will be designated in the following as $O^-[N]$. Obviously a charge transfer from oxygen anions (eq 1) must have taken place during the formation of the electron deficient paramagnetic oxygen species.[14,16] There is, however, no EPR evidence for the resulting electron acceptor which was previously observed by Ito et al.[13] In the present

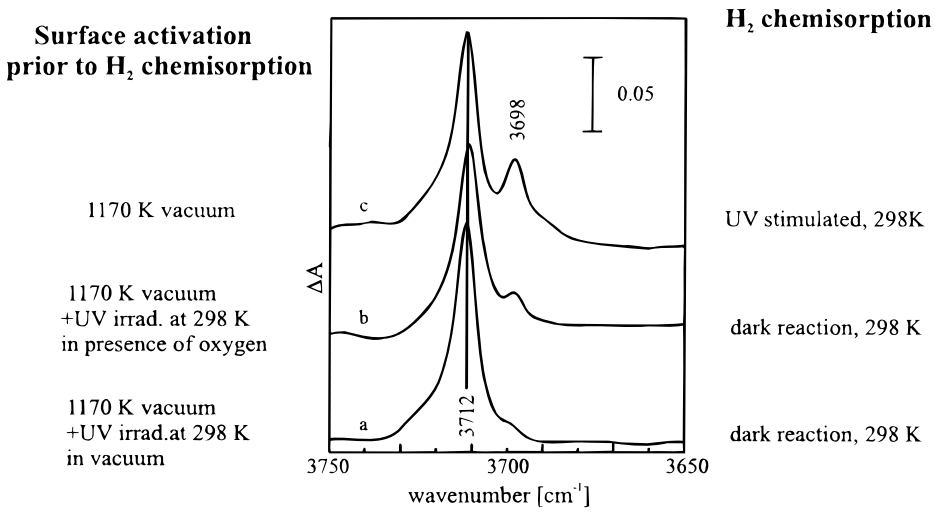

Figure 1. IR spectra of isolated free OH groups on the surface of MgO under diverse experimental conditions of activation and H_2 chemisorption.

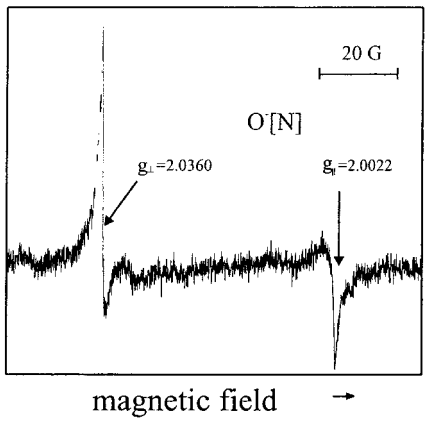

Figure 2. EPR spectrum of the electron deficient surface oxygen anion species O^-[N] on MgO under dynamic high-vacuum conditions.

study either diamagnetic products such as F_S^0 centers or paramagnetic species which are not detectable under the given experimental conditions (=77 K) have to be assumed. The intensity of the O^-[N] signal may considerably be raised by the addition of molecular oxygen during irradiation (Figure 3a).

Furthermore, there is, owing to the overlap of signals, a complex envelope at high field. As may be shown by the study of the microwave saturation behavior, they originate from two different species. One of them gives rise to three signal components which reflect the anisotropy of an ozonide anion in agreement with literature data.[34,35] The additional resonance at $g = 2.007$ corresponds to the g_{yy} component of a superoxide anion signal. It is accompanied by two corresponding g_{zz} components located at $g = 2.085$ and $g = 2.073$, whereas the g_{xx} component is obviously buried under the above-mentioned ozonide signal. The presence of two g_{zz} resonances indicates the presence of two O_2^- types which are differently coordinated by surface cations. They are not identical with previously reported superoxide anions on the surface of MgO nanoparticles.[28]

All surface oxygen species presented here are stable under dynamic vacuum conditions at room temperature. Their characterization by EPR is in good agreement with results of Ito et al.[16] obtained on samples which were prepared and UV activated in different ways. Addition of oxygen gas does not alter the signal intensities to any significant extent. On the other hand, ozonides and O^- react instantaneously with hydrogen even at liquid nitrogen temperature. An increase in temperature from

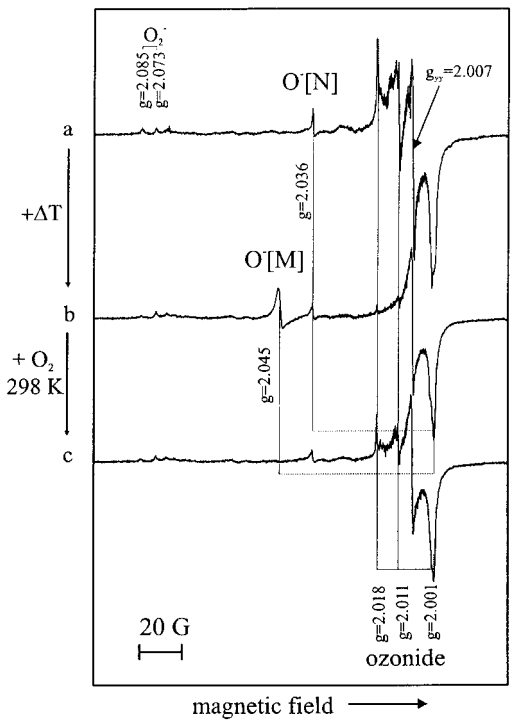

Figure 3. EPR spectra of MgO after (a) UV activation in the presence of O_2, (b) a plus 10 min thermal treatment at 373 K under dynamic vacuum conditions, and (c) b plus admission of O_2 at room temperature and subsequent evacuation.

298 K to 373 K for 10 min under dynamic vacuum gives rise to the destruction of the ozonide signal and the formation of a new O^- species at $g_\perp = 2.045$ (designated in this work as O^-[M]). At the same time the signal related to O^-[N] undergoes a slight intensity decrease. The characteristic shape of the superoxide anion resonances in the high-field region (g_{yy} and g_{xx}) are now less overlapped by other signal contributions and, therefore, clearly visible (Figure 3b). The formation of O^-[M] is fully reversible: addition of oxygen at the original pressure and temperature makes the signal of O^-[M] disappear and restores that of the respective ozonide. Obviously O^-[M] reacts instantaneously with O_2 according to eq 7. There is a funda-

$$(O_M^-)_S + O_2 \overset{O_2}{\longleftrightarrow} O_3^- \qquad (7)$$

mental mechanistic difference in the formation process of O^-[N]

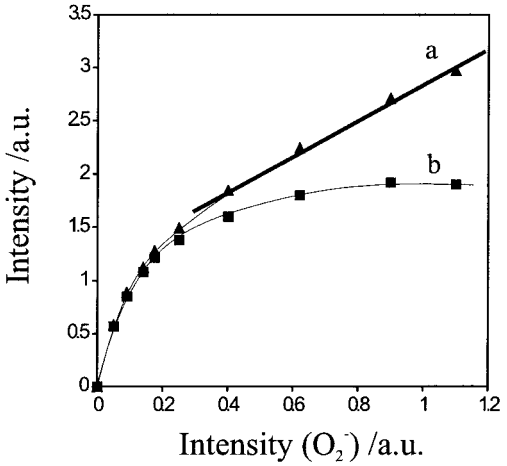

Figure 4. Correlation of the signal intensities related to O^- and O_3^- on one hand and O_2^- on the other: (a) $I(O^-) + I(O_3^-)$ versus $I(O_2^-)$; (b) $I(O^-)$ versus $I(O_2^-)$.

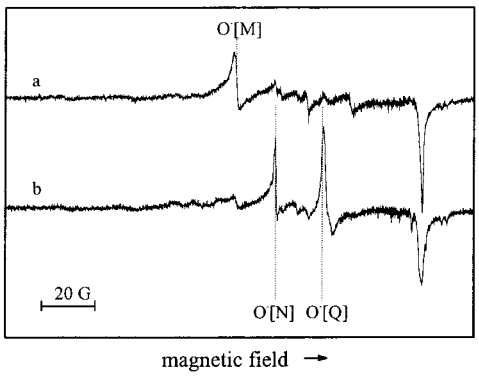

Figure 5. EPR spectra of MgO after surface color center bleaching by N_2O. (a) F_S^+(H) is transformed into O^- [M]; (b) F_S^+[A] and F_S^+[B] are transformed into O^-[N] and O^-[Q].

and O^-[M]. O^- [N] is directly obtained by polychromatic UV excitation of a low-coordinated O^{2-} surface anion in vacuo as well as in the presence of molecular oxygen (Figures 2 and 3). In contrast, the formation of O^-[M] necessarily implies the presence of oxygen. As a primary product ozonide anions appear which decompose thermally into O^-[M] and molecular oxygen. The electron acceptor in the process of O^- and O_3^- formation is molecular oxygen. The resulting coupling of eqs 1 to 3 is demonstrated by the diagram in Figure 4, which correlates the EPR signal intensities of O^- and O_3^- with that of O_2^-, the parameter being the exposition time of the sample to UV light.

(3) Bleaching of Color Centers with N_2O. UV irradiation of a dehydroxylated defective MgO surface in the presence of 100 mbar H_2 at room temperature leads to the formation of paramagnetic surface color centers (predominantly of the type F_S^+(H)), which have been discussed extensively in the past.[22,23,36] The EPR signal of the blue colored sample is in good agreement with those reported on other high surface area MgO materials.[22,23,36] The structure of the signal indicates that there is a dipolar magnetic interaction between the electron spin density of the color center and the nuclear moment of a nearby proton.[23,36]

Bleaching the color centers with 0.5 mbar N_2O destroys the respective signal within 1 min and, according to eq 5, gives rise to the formation of O^-[M] (Figure 5a). O^-[N] is formed to a considerably lesser extent (around 10% of the intensity of M). These observations are absolutely independent of the temperature applied during the bleaching process (298 and 85 K). O^-[M] appears to be stable under dynamic vacuum conditions on a time scale of hours.

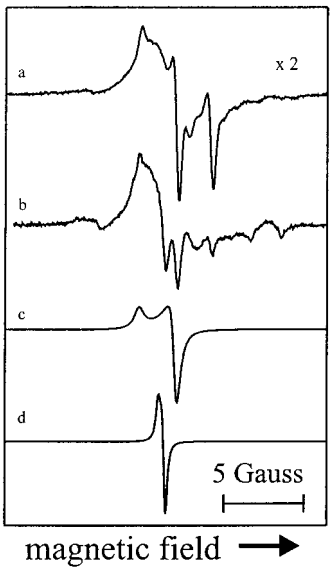

Figure 6. Experimental (a and b) and simulated (c and d) color center signals of MgO: (a) UV irradiation of MgO in the presence of H_2 leading to formation of predominantly F_S^+(H) centers; (b) reaction of O^-[M] with H_2 leading to the formation of F_S^+[A] and F_S^+[B].

In section 2 the genesis of O^-[M] and O^-[N] was described. Both radical species react instantaneously with hydrogen according to

$$O_S^- + H_2 \rightarrow (O_SH)^- + \dot{H} \qquad (8)$$

The EPR spectrum (Figure 6b) unambiguously evidences that the resulting H atom gives rise to a further reaction step. It initiates the transformation of previously not involved anion vacancies into surface color centers. The shape of the respective signal strongly differs from that in Figure 6a, and its integral signal intensity amounts to 30−50%. The variation of the microwave power applied during the experiment of Figure 6b indicates the presence of predominantly two F_S^+ centers, which have already been suggested previously[36,41] and will be denoted here as F_S^+[A] and F_S^+[B]. A simulation procedure carried out on this basis provides the contour of the two species (Figure 6c,d). The presence of a superhyperfine splitting originating from dipolar magnetic interaction with a nearby proton, as in Figure 5a, can be excluded. The tentatively obtained g values are presented in Table 1.

The presence of two new types of F_S^+ color centers strongly urges one to carry out another bleaching experiment by N_2O addition. Figure 5b shows the result: two further types of O^- are produced that are fundamentally different from O^-[M] (Figure 5a). One of them is identical with O^-[N] (Figure 3a−c) observed after irradiation of the MgO sample under a vacuum or in the presence of O_2. The other one has never been seen before and is designated here by O^-[Q] (with $g_\perp = 2.024$ and $g_\parallel \approx g_e$). At room temperature it reacts with H_2 similar to the other species O^-[N] and O^-[M]. Different from them it does not react with H_2 at 77 K. The observed O^- spectra do not exhibit any effect due to superhyperfine interaction with hydroxyl groups. This is corroborated by the fact that isotope substitution H/D does not alter the signal contour to any significant extent.

TABLE 1: *g*-values of the Observed Radical Species

experimental conditions		predominant paramagnetic species	**g** matrix components		
UV excitation of low-coordinated anions	UV, vacuum	O^-[N]	$g_\perp = 2.036$	$g_\parallel = 2.002$	
	UV, O_2	O^-[N]	$g_\perp = 2.036$	$g_\parallel = 2.002$	
		O_3^-	$g_{xx} = 2.0014$	$g_{yy} = 2.018$	$g_{zz} = 2.012$
		O_2^-	$g_{xx} = 2.0023$	$g_{yy} = 2.007$	$g_{zz} = 2.082/2.086$
	O_3^-, $\Delta T > 298$ K	O^-[M}	$g_\perp = 2.046$	$g_\parallel = 2.002$	
"filling" of anion vacancies	UV, H_2	F_S^+(H)	$g_\perp = 1.9997$	$g_\parallel = 2.0013$	
	F_S^+(H) + N_2O	O^-[M]	$g_\perp = 2.046$	$g_\parallel = 2.002$	
	O^-[M] + H_2	F_S^+[A]	$g_\perp = 2.0004$	$g_\parallel = 2.0017$	
		F_S^+[B]	$g_\perp = 2.0007$	$g_\parallel = 2.0010$	
	F_S^+[A]/F_S^+[B] + N_2O	O^-[N]	$g_\perp = 2.036$	$g_\parallel = 2.002$	
		O^-[Q]	$g_\perp = 2.024$	$g_\parallel = 2.002$	

Discussion

Contrary to previous presumptions[37,38] thermal treatment of polycrystalline MgO in vacuo does not result in the formation of O^- species which survive at room temperature in the dark. These species, designated here as O^-[N], are, however, observed by EPR spectroscopy after UV irradiation (Figure 2). They react instantaneously—even at 77 K—with H_2 according to homolytic cleavage (eq 8). The resulting IR active surface OH group has not been observed owing to the comparatively low sensitivity of IR spectroscopy. UV activation of MgO in the presence of O_2 enhances the intensity of the above-mentioned EPR signal by a factor of about 5, since the charge separation related to the UV activation (eq 2) is stabilized by the consumption of the resulting electron in the course of O_2^- formation. Under these conditions the surface OH group emerging from homolytic H_2 cleavage becomes accessible to IR spectroscopy (Figure 1b, band at 3698 cm^{-1}). The respective OH group further gains intensity if the UV activation takes place in a H_2 atmosphere (Figure 1c). The major reaction product under these conditions are surface color centers which were previously discussed.[23,28,36] It has to be emphasized that the centers where homolytic H_2 splitting occurs fundamentally differ from those where heterolytic H_2 splitting takes place, even though both necessarily require low-coordinated anion positions. The respective band positions at 3698 and 3712 cm^{-1} (Figure 1), respectively, are significantly separated from each other.

In addition to O^- stabilization the O_2 presence during UV activation provokes another surface reaction (Figure 3a), namely, the ozonide formation. A quantitative analysis of the intensities of the O^- and O_3^- signals on one hand and the O_2^- signal on the other is possible on the basis of eqs 1 and 3. The corresponding processes provide an electron each which—most likely—has to be adopted by O_2 as the common electron acceptor. In agreement with this assumption the correlation between the following pairs of signal intensity, $I(O^-)$ and $I(O_2^-)$ (Figure 4a), and $I(O^-) + I(O_3^-)$ and $I(O_2^-)$ (Figure 4b), were examined with the time of polychromatic UV irradiation ($\lambda >$ 200 nm) as parameter. There is a nonlinear correlation in the initial phase until 5 min. Later on a linear correlation is observed for (b) only. This confirms that the two parallel and independent from each other occurring UV induced electron-transfer processes − O^-[N] and O_3^- formation according to eqs 1 and 3, respectively, give rise to the EPR spectrum of Figure 3a. The linear correlation also excludes a mechanism in terms of secondary formation steps such as photodissociation intermediates.[14] The UV induced ozonide formation was previously explained by the following subsequent reaction steps:[15]

$$V_S^{2-} + h\nu_{UV} \rightarrow V_S^- + e^- \quad (9)$$

$$V_S^- + O_2 \rightarrow O_3^- \quad (10)$$

where V_S^{2-} stands for a single surface cation vacancy which is made up of the remaining anions after removal of a surface cation. This model is not in agreement with our experimental data. As shown in Figure 3b, O^-[M] originates from O_3^- via thermal treatment. On the other hand O^-[M], which corresponds to V_S^- cannot be produced directly by UV excitation. This unambiguously evidences that the UV quanta and O_2 molecules as reactants must simultaneously be present at the reactive site V_S^{2-}:

$$V_S^{2-} + O_2 + h\nu_{UV} \rightarrow O_3^- + e^- \quad (11)$$

In light of the previous discussions, we are led to the following conclusions: The O^-[N] species is related to a simple low-coordinated corner or edge anion, whereas the O^-[M] species has to be considered as a paramagnetic constituent of a cation vacancy.

The O^- sites in question are certainly no adatoms. This is evidenced by IR and EPR spectroscopy: The OH group related to homolytic H_2 splitting absorbs at 3698 cm^{-1}, i.e., significantly below the value attributed to one-coordinated OH groups (>3740 cm^{-1}).[27]

Under the experimental conditions of Figure 1c not only heterolytic and homolytic H_2 splitting occurs at the same time, the newly formed hydride groups are simultaneously subject to a UV induced redox reaction:[22,28]

$$F_S^{2+} + {}^1/_2H^- \xrightarrow{h\nu} F_S^+(H) + {}^1/_2H^+ \quad (12)$$

The resulting F_S^+(H) center has previously been studied by EPR and ENDOR spectroscopy.[23,36] Indirectly it may also be observed by IR spectroscopy via the interaction of the OH group with the color center.[31] The specific local ionic geometry of this paramagnetic defect was described[22] in terms of an anion vacancy formed by three cations, which remains when the corner oxygen anion is removed.

The process of bleaching the surface color center in question by N_2O gives rise to the replacement of the color center electrons by O^- radical anions.[18] The resulting surface species is identical to O^-[M] obtained by UV induced ozonide formation (eq 3) and subsequent thermal splitting according to the back-reaction in eq 7 (Figure 3a,b). It reacts with H_2, giving rise to an OH group and a neutral H atom which—as an uncharged particle—is likely to be mobile on the surface. Even though color centers were already formed in a previous reaction step (Figure 6a) and then occupied by an O^- ion (Figure 5a), there are still surface anion vacancies available. They act as a trap for the electron of

the mobile H atom.[39] The two resulting color centers (F_S^+[A] and F_S^+[B], Figure 6 c,d, respectively) strongly differ from those previously obtained (F_S^+(H), Figure 6a), which is in contrast with findings of Tench[18] (Figure 5b). The respective **g** matrix components are in agreement with literature data related to completely different preparative techniques of surface color center formation: (a) γ irradiation of MgO;[40] (b) deposition of neutral alkaline and alkaline earth atoms as reducing agents on the MgO surface ("additional coloring").[41,42] Although the color center formation necessarily involves the appearance of a proton (eq 13), which is likely to remain in the vicinity of the color center, there are no superhyperfine coupling effects observed in the spectrum (Figure 6b). As is to be expected, the repeated addition of N_2O transforms these color centers into O^- types (Figure 5b) which differ from each other (O^-[N] and O^-[Q]) and from that observed after the first bleaching step with N_2O (O^-[M], Figure 5a). According to eq 6 the $g_\perp$ value is inversely proportional to the stabilizing crystal field[25,43] which itself is proportional to the number of coordinating cations. Thus, a rough estimate shows that the coordination of O^-[Q] is by a factor of 2 higher than that of O^-[M]. This would lead to the puzzling result that O^-[Q] is a subsurface species. Two of the three O^- types are also known from bleaching of color centers obtained by "additional coloring".[41] Most interestingly, the presence of Mg atoms as reducing agent on the surface gives rise to O^-[N], whereas K atoms lead to O^-[M].[42]

At first sight the two electronic excitation wavelengths of 230 and 270 nm[7] suggest the attribution of O^-[M] and O^-[N] to edge (four-coordinated) and corner (three-coordinated) oxygen anions, respectively. This is, however, in conflict with the fact that both wavelengths give rise to the appearance of O^-[N], whereas O^-[M] requires a wavelength around 300 nm and the presence of oxygen gas.[44]

Obviously the simple model of five-, four-, and three-coordinated oxygen anions, surface cation vacancies, and surface color centers does not meet with the requirements of the genesis of O^- species. An alternative explanation goes back to the beginnings of surface defect studies. Lunsford and Jayne[45] introduced the model of a cation−anion divacancy which is energetically much less costly than a pair of isolated vacancies. Recent theoretical calculations were performed, reporting that the tub form (the two removed ions are nearest neighbors in the surface) is more stable than the pit form (one of the removed ions is in the surface, the other one below).[46]

Double vacancies combine the properties of anion vacancies F_S^{2+} and of cation vacancies V_S^{2-} (Figure 7). In particular the two types of O^-[M] genesis may consistently be interpreted on the basis of the presence of divacancies. The insertion of O^- into an edge vacancy according to eqs 4 and 5 provides a cation vacancy incorporating an O^- in its framework (Figure 7, left). Precisely the same configuration is obtained after long-wavelength UV induced ozonide formation at a single cation vacancy and subsequent thermal decomposition (Figure 7, right). The observation of O^-[M] as the product of both reaction paths thus strongly supports the assumption of divacancies.

Another interesting property of double vacancies was worked out by theoretical calculations: The related paramagnetic color center (F_S^+) is stable, whereas the diamagnetic version (F_S^0) is not,[46] in perfect agreement with our previous IR spectroscopic detection of F_S^+(H) centers.[28,31] There is unambiguous evidence that the paramagnetic double vacancy cannot be transformed into a diamagnetic F_S^0(H) center. This is in clear contradiction to recent findings[23] that the abundance of diamagnetic color centers is considerably higher than that of the paramagnetic ones.

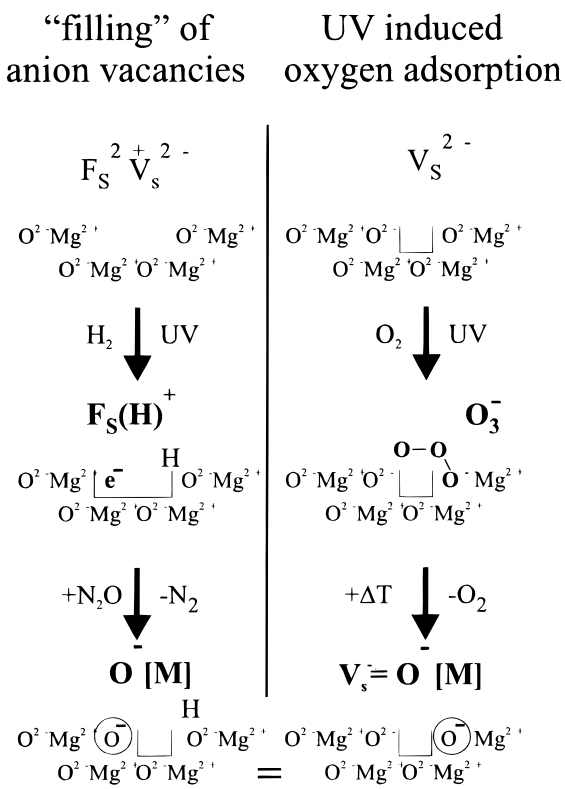

Figure 7. Schematic representation of the formation of O^-[M] on two fundamentally different reaction paths starting with anion−cation divacancies and with a single cation vacancy, respectively.

Conclusion

In general highly dispersed metal oxides exhibit a more or less broad distribution for each type of surface site. The present paper demonstrates that the surface of MgO nanoparticles originating from chemical vapor deposition hosts diverse types of reactive centers such as O^-, vacancies, and color centers and that each type is represented only by a limited number of local structures, in general not more than three. Therefore, this material is particularly well-suited as a model substance for surface studies aiming at the correlation of structure and reactivity. Thus, there are two fundamentally different surface effects of UV excitation for MgO in an O_2 atmosphere. Polychromatic UV light (λ > 200 nm) initiates two charge-transfer processes, one ending up with O^- and the other one with O_3^-, both of which were identified by EPR spectroscopy. The wavelength dependence might help to elucidate the reaction mechanisms in terms of the specific local surface structures involved.

Another important issue of the present study is the fascinating system of parallel and consecutive surface reactions between the subsequent levels of surface states: anion vacancies (reacting with H^- and H atoms as reducing agent), color centers (bleached by N_2O), O^- species (splitting H_2 homolytically and providing H atoms as reducing agent), and then again color centers. The discrimination of the products of parallel reactions on each level was possible on the basis of EPR experiments which also provided relevant data contributing to our present knowledge related to the structure−reactivity correlation. In the preliminary surface model developed in this paper the anion−cation divacancy plays a very prominent role. It has, however, still to be controlled and implemented by another absolutely indepen-

dent analytical tool such as FTIR spectroscopy, which is based on surface OH groups as IR active probes. They are known to react sensitively on physical and chemical changes in their immediate environment.[28,31]

Acknowledgments. Considerable financial support from the Fonds zur Förderung der Wissenschaftlichen Forschung (contract no. P11542-CHE and the Max-Buchner-Forschungs-Stiftung (contract no. H-00027/95) is gratefully acknowledged.

References and Notes

(1) Henrich, V. E.; Cox, P. C. *The Surface Science of Metal Oxides*; Cambridge University Press: Cambridge, U.K., 1996; and references cited therein.

(2) Zecchina, A.; Scarano, D.; Galletto, P.; Lamberti, C. *Nuovo Cimento* **1997**, *19*, 1773, and references cited therein.

(3) Colbourn, E. A.; Mackrodt, W. C. *Surf. Sci.* **1982**, *117*, 571.

(4) Shluger, A. L.; Gale, J. D.; Catlow, C. R. A. *J. Phys. Chem*. **1992**, *96*, 10389.

(5) Pacchioni, G.; Pescarmona, P. *Surf. Sci.* **1998**, *413*, 657.

(6) Shluger, A. L. *Phys. Rev. B* **1999**, *59*, 2417.

(7) Garrone, E.; Zechina, A.; Stone, F. S. *Philos. Mag. B* **1980**, *42*, 683.

(8) Coluccia, S.; Tench, A. J. In *Proceedings of the 7th International Congress on Catalysis*, Tokyo, 1980; Seyama, T., Tanabe, K., Eds.; Kodansha: Tokyo, 1981; Vol. B, p 1154.

(9) Wu, M. C.; Truong, C. M.; Coulter, K.; Goodman, D. W. *J. Am Chem. Soc*. **1992**, *114*, 7565.

(10) Orlando, R.; Millini, R.; Perego, G.; Dovesi, R. *J. Mol. Catal*. **1997**, *A119*, 2653.

(11) Lunsford, J. H. In *Handbook of Heterogeneous Catalysis*; Ertl, G., Knözinger, H., Weitkampp, J., Eds.; VCH: Weinheim, 1997; Vol. 4, p 1843.

(12) Goto, A.; Aika, K. *Bull. Chem. Soc. Jpn*. **1998**, *71*, 95.

(13) Ito, T.; Kawanami, A.; Toi, K.; Shirakawa, T.; Tokuda, T. *J. Phys. Chem*. **1988**, *92*, 3910.

(14) Iwamoto, M.; Lunsford, J. H. *Chem. Phys. Lett*. **1979**, *66*, 48.

(15) Tench, A. J.; Kaufherr, N. *Proc. Int. Congr. Catal. 6th* **1977**, *1*, 182.

(16) Ito, T.; Kato, M.; Toi, K.; Shirakawa, T.; Ikemoto, I.; Tokuda, T. *J. Chem. Soc., Faraday Trans. 1* **1985**, *81*, 2835.

(17) Che, M.; Tench, A. J. *Adv. Catal*. **1983**, *23*, 1.

(18) Tench, A. J.; Lawson, T.; Kibblewhite, J. F. J. *J. Chem. Soc., Faraday Trans. 1* **1972**, *68*, 1169.

(19) Williamson, N. B.; Lunsford, J. H.; Naccache, C. *Chem. Phys. Lett*. **1971**, *9*, 33.

(20) Harkins, C. G.; Shang, W. W.; Leland, T. W. *J. Phys. Chem*. **1969**, *73*, 100.

(21) Martra, G.; Coluccia, S.; Knözinger, E. Unpublished work.

(22) Giamello, E.; Paganini, M. C.; Chiesa, M.; Coluccia, S.; Martra, G.; Murphy, D.; Pacchioni, G. *Surf. Sci.* **1999**, *421*, 246.

(23) Murphy, D. M.; Farley, R. D.; Purnell, I. J.; Rowlands, C. C.; Yacob, A. R.; Paganini, M. C.; Giamello, E. *J. Phys. Chem. B* **1999**, *103*, 1944.

(24) Che, M.; Tench, A. J. *Adv. Catal*. **1982**, *31*, 77.

(25) Brailsford, J. R.; Morton, J. R. *J. Chem. Phys*. **1969**, *51*, 4794.

(26) Becker, A.; Benfer, S.; Hofmann, P.; Jacob, K.-H.; Knözinger, E. *Ber. Bunsen-Ges. Phys. Chem*. **1995**, *99*, 1328.

(27) Knözinger, E.; Jacob, K.-H.; Singh, S.; Hofmann, P. *Surf. Sci*. **1993**, *290*, 388.

(28) Diwald, O.; Hofmann, P.; Knözinger, E. *Phys. Chem. Chem. Phys*. **1999**, *1*, 713.

(29) Coluccia, S.; Boccuzzi, F.; Ghiotti, G.; Mirra, C. *Z. Phys. Chem. (Munich)* **1980**, *121*, 141.

(30) Coluccia, S.; Boccuzzi, F.; Ghiotti, G.; Morterra, C. *J. Chem. Soc., Faraday Trans. 1* **1982**, *78*, 2111.

(31) Diwald, O.; Martra, G.; Knözinger, E. *J. Chem. Phys*. **1999**, *111*, 6668.

(32) Duley, W. W. *Philos. Mag. B* **1984**, *49*, 159.

(33) Yanagisawa, Y.; Huzimura, R. *J. Phys. Soc. Jpn*. **1981**, *50*, 209.

(34) Tench, A. J. *J. Chem. Soc., Faraday Trans*. **1972**, *68*, 1181.

(35) Che, M.; Giamello, E.; Tench, A. J. *Colloids Surf*. **1985**, *13*, 231.

(36) Giamello, E.; Paganini, M. C.; Murphy, D. M.; Ferrari, A. M.; Pacchioni, G. *J. Phys. Chem*. **1997**, *101*, 971.

(37) Boudart, M.; Delbouille, A.; Derouane, E. G.; Indovina, V.; Walters, A. B. *J. Am. Chem. Soc*. **1972**, *94*, 6622.

(38) Knözinger, E.; Jacob, K. H.; Hofmann, P. *J. Chem. Soc., Faraday Trans. 1* **1993**, *89*, 1101.

(39) Smith, D. R.; Tench, A. J. *Chem. Commun*. **1968**, 1113.

(40) Nelson, R. L.; Tench, A. J.; Harmsworth, B. J. *Trans. Faraday Soc*. **1967**, *63*, 1427.

(41) Giamello, E.; Ferrero, A.; Coluccia, S.; Zecchina, A. *J. Phys. Chem*. **1991**, *95*, 9385.

(42) Murphy, D.; Giamello, E. *Mol. Eng*. **1994**, *4*, 147.

(43) Kollrack, R. *J. Catal*. **1968**, *12*, 321.

(44) Sterrer, M. Master Thesis, Technical University of Vienna, **1999**, to be published.

(45) Lunsford, J. H.; Jayne, J. P. *J. Phys. Chem*. **1966**, *70*, 3463.

(46) Ojamäe, L.; Pisani, C. *J. Chem. Phys*. **1998**, *109*, 10984.